e-*Blood*

Tumor suppressor genes FHIT and WWOX are deleted in primary effusion lymphoma (PEL) cell lines

Debasmita Roy,[1,2] Sang-Hoon Sin,[2] Blossom Damania,[1,2] and Dirk P. Dittmer[1,2]

[1]Curriculum in Genetics and Molecular Biology and [2]Department of Microbiology and Immunology, UNC Lineberger Comprehensive Cancer Center, UNC Center for AIDS Research, University of North Carolina at Chapel Hill, Chapel Hill, NC

Primary effusion lymphoma (PEL) is a diffuse-large B-cell lymphoma with poor prognosis. One hundred percent of PELs carry the genome of Kaposi sarcoma–associated herpesvirus and a majority are coinfected with Epstein-Barr virus (EBV). We profiled genomic aberrations in PEL cells using the Affymetrix 6.0 SNP array. This identified for the first time individual genes that are altered in PEL cells. Eleven of 13 samples (85%) were deleted for the fragile site tumor suppressors *WWOX* and *FHIT*. Alterations were also observed in the *DERL1*, *ETV1*, *RASA4*, *TPK1*, *TRIM56*, and *VPS41* genes, which are yet to be characterized for their roles in cancer. Coinfection with EBV was associated with significantly fewer gross genomic aberrations, and PEL could be segregated into EBV-positive and EBV-negative clusters on the basis of host chromosome alterations. This suggests a model in which both host genetic aberrations and the 2 viruses contribute to the PEL phenotype. (*Blood*. 2011;118(7): e32-e39)

Introduction

Primary effusion lymphoma (PEL) is a postgerminal center (GC), diffuse-large B-cell lymphoma (DLBCL) with poor prognosis. It is characterized by an accumulation of tumor cells in the serous cavities of the body and therefore was initially referred to as body cavity–based lymphoma. Since then, isolated instances of solid, lymph node-associated variants have also been described.[1] Morphologically, PELs are pleiomorphic and exhibit heterogeneity in cell size and nuclear shape. PEL is an AIDS-defining malignancy, and it usually manifests itself in conjunction with Kaposi sarcoma (KS). However, PEL has also been diagnosed in HIV-negative patients experiencing severe immune-suppression after organ transplantation. PEL is unique histologically as well as in its expression of immunophenotypic markers, mRNA, and microRNA profiles.[2-4] As expected for cancer cells, PEL cell lines show gross chromosomal alterations.[5,6] Genomewide high-resolution analyses of copy number variants (CNVs) and loss of heterozygosity (LOH), which would aid our understanding of PEL, have not been reported.

All PELs are infected with KS-associated herpesvirus (KSHV).[2] KSHV is also the causative agent for KS[7] and the plasmablastic variant of multicentric Castleman disease.[8] KSHV is required for PEL survival; a subset of viral proteins as well as all viral microRNAs are consistently expressed in all PEL cells.[9] Most PELs are also coinfected with EBV, and this results in altered host mRNA transcription compared with EBV-negative PEL cells.[10] It has been reported that on overexpression of a dominant-negative form of the EBV EBNA2 protein, some EBV-positive PELs cease to proliferate.[11] Yet the contribution of EBV to PEL development remains unclear because both EBV-positive and EBV-negative PEL cell lines grow equally well in culture and form tumors with equal efficiency in immune-deficient mice.[12,13]

Cancer is thought to arise in a multistep fashion, although not necessarily in a linear manner, in which each step provides a selective advantage in terms of cell proliferation and cell survival in the tumor microenvironment. This leads to cancer type–specific genome signatures such as the classic "Philadelphia" t(9;22)(q34; q11) translocationm resulting in oncogenic BCR/ABL gene fusion in chronic myelogenous leukemia.[14] These signatures in turn provide tumor cell–specific targets for therapy (eg, use of imatinib mesylate/Gleevec in chronic myelogenous leukemia). In non–virus-associated cancers, each step in the pathway involves activating or inhibitory mutations in cellular oncogenes or tumor suppressors, respectively. In virus-associated cancers, the virus contributes to one or multiple steps along this pathway, thus reducing the need for specific mutations in host oncogenes or tumor suppressor genes.

Chromosomal imbalances and genomic instability comprise a major contributing factor in malignant diseases. Unlike other lymphomas, no signature translocation or single gene mutation has been associated with PEL to date. The p53 tumor suppressor protein appears functional in PEL cell lines,[15] the Myc locus un-rearranged, although the protein is unusually stable,[16] and no amplifications or deletions are reported for Bcl-2,[2] Bcl-6,[17] Ras,[2] the catalytic subunit of PI3K,[18] phosphatase with tensin homolog or p16/INK4.[18] We therefore used the Affymetrix 6.0 single nucleotide polymorphism (SNP)–based microarray to conduct comparative genomic hybridization (CGH) to look at the global genomic profile of PEL cells. This identified PEL-specific gene alterations in the fragile site tumor suppressor genes, fragile histidine triad (*FHIT*) and WW-domain containing oxidoreductase (*WWOX*), which were deleted in 11 of 13 (85%) and 12 of 13 (92%) samples, respectively ($P \leq .0005$). In addition, we observed alterations in other key signaling pathways albeit at a lower frequency. Because a

Submitted December 22, 2010; accepted June 3, 2011. Prepublished online as *Blood* First Edition paper, June 17, 2011; DOI 10.1182/blood-2010-12-323659.

The online version of this article contains a data supplement.

The publication costs of this article were defrayed in part by page charge payment. Therefore, and solely to indicate this fact, this article is hereby marked "advertisement" in accordance with 18 USC section 1734.

subset of PEL are coinfected with EBV in addition to KSHV, we asked whether EBV influenced overall genomic instability or was associated with genomic alterations in specific genes. EBV-negative PEL cell lines exhibited significantly increased genomic amplifications compared with EBV-positive, suggesting that the presence of EBV contributes to genomic stability.

Methods

Cell culture

The PEL cell lines used in the study are shown in Table 1. All PEL and non-PEL lymphoma and leukemia cells (BJAB, KSHV-BJAB, DG75, BL5, BL8, Thp1, and Thp1-KSHV) were cultured in RPMI 1640 supplemented with 100 μg/mL streptomycin sulfate, 100 U/mL penicillin G (Life Technologies), 2mM L-glutamine, 0.05mM 2-mercaptoethanol, 0.075% sodium bicarbonate, 1 U/mL IL-6 (PeproTech Inc), and 10% FBS and were maintained at 37°C in 5% CO_2. All nonlymphoma cells (E1-TIVE, L1-TIVE, HEK293, and HEK293-KSHV) were maintained in DMEM supplemented with 100 μg/mL streptomycin sulfate, 100 U/mL penicillin G, and 10% FBS.

DNA extraction and CGH

Genomic DNA was extracted with the Wizard Genomic DNA Purification Kit (Promega) as per the manufacturer's protocol. Signature profiles were obtained with the 6.0 GeneChip Human Mapping Array that uses > 906 600 known SNP and 946 000 CNV markers (Affymetrix). As control we used the older 500K Affymetrix array. The SNP and CNV data have been deposited in the NIH GEO Datasets archives: GSE25839 and GSE28684.

Data analysis

All analyses were performed with the Partek Genomics Suite v6.0 (Partek Inc). Raw CGH data (.CEL files) were imported and adjusted for background with the use of the Robust Multi-array Average algorithm. CNV was determined by generating copy number values with the use of the Genomic Segmentation algorithm with preset program parameters and was compared with the 270 HapMap baseline (Version 122809) available at http://www.affymetrix.com/support/technical/sample_data/genomewide_snp6_data.affx. Gene lists were generated by determining regions of significance (by estimating *t* statistics for each probe adjusted for multiple comparisons by MAT algorithm) in multiple samples and annotated with the NCBI Reference Sequence database.[19] Further statistical analyses used the R v2.11.1 statistical software environment (R Project for Statistical Computing).

Real-time quantitative PCR analysis

We used real-time quantitative PCR (qPCR) to verify some candidate genes. We selected primers following criteria outlined by D'Haene et al[20] from RTprimerDb (www.rtprimerdb.org). Primer sequences used were *DERL1* (forward: 5′-TACTCCAGCTACACAAAG-3′; reverse: 5′-AATGAGATACGAGGGTTG-3′), *FHIT* (forward: 5′-CCAGTGGAGCGCTTCCAT-3′; reverse: 5′-TCCACCACTGTCCCGACTCT-3′), *GRID2* (forward: 5′-GCATTTCAGTGTTTTGAAAATTG-3′; reverse: 5′-CCAGTCTGGGCAAACTCATT-3′), *WWOX* (forward: 5′-GCAATGAAGGCAACAAAGT-3′; reverse: 5′-TTAAAAGACCTGGGGGAAT-3′), and LANA78 (forward: 5′-GGAAGAGCCCATAATCTTGC-3′; reverse: 5′-GCCTCATACGAACTCGAGGT-3′). Cycling conditions were 95°C for 10 minutes followed by 45 cycles of 95°C for 15 seconds and 60°C for 1 minute followed by melting curve analysis on a Roche LC480 Lightcycler. All reactions were conducted in 5 technical replicates. Purified normal human genomic DNA (Roche) was used as positive control, and water served for the nontemplate negative control. A standard curve was generated with serial (1:4) dilutions of human genomic DNA, starting at 8 μg/mL concentration, against the individual primers. We used robust regression and normalized by primer followed by human diploid DNA (Roche) to obtain relative copy number changes for each sample relative to normal diploid human DNA.

Table 1. Summary of PEL samples

Name	KSHV	EBV	p53 Status	Type	Original description
AP2	+	+	K139E;	PEL	Carbone et al[21]
AP5	+	+	R181P	PEL	Carbone et al[22]
BC1	+	+	Wild type	PEL	Cesarman et al[23]
BC2	+	+	Wild type	PEL	Cesarman et al[23]
BC3	+	–	Wild type	PEL	Arvanitakis et al[24]
BC5	+	+	Wild type	PEL	Guasparri et al[25]
BCBL1	+	–	S262 insertion	PEL	Komanduri et al[26]
BCLM	+	–	Wild type	PEL	Ghosh et al[27]
BCP1*	+	–	M246I	PEL	Boshoff et al[28]
HHB2	+	–	Wild type	PEL	Gradoville et al[29]
JSC1	+	+	Wild type	PEL	Cannon et al[30<zrefx]
TY1	+	–	S262 insertion; M246I	PEL	Katano et al[31]
VG1*	+	–	Wild type	PEL	Brander et al[32]

*Isolated from HIV-negative patient.

Results

Genetic signature of PEL: FHIT and WWOX

With the use of the high-resolution Affymetrix 6.0 and the 500K SNP array we assessed the genomic signatures of virtually all available PEL cell lines. We used cell lines, because they form a renewable resource and have been characterized phenotypically for growth in culture and tumorigenicity in mice, in vitro and in vivo drug susceptibility, mRNA transcription, miRNA expression, p53 status, and other markers (Table 1 and references therein).[3,4,12,13,15] Although the samples displayed a high degree of variability in their genomic signatures, with the use of principle component analysis (PCA) we found that most PEL cell lines (with the exception of JSC1) form a tight cluster. PCA reduced the variability of the data to 3 main and independent components. The first principle component (PC1) accounted for 14.9% of variability, PC2 and PC3 accounted for 12.2% and 11.7%, respectively. As expected PEL cells could easily be distinguished from non-PEL control cell lines (including KSHV-positive endothelial cells that also form xenograft tumors in mice) on the basis of genomic alterations (Figure 1).

With the use of PCA of only the PEL data we found that all PEL cell lines clustered together irrespective of whether they were grown in culture or as xenografts in mice (data not shown). This showed that PEL cell lines form tumors in mice without acquiring additional mutations in vivo. This phenotype would be expected for a monoclonal tumor, as PEL is believed to be. For our detailed analysis, we excluded the samples from xenografts, to avoid the bias of repeat sampling of some PEL lines, and exclusively focused on the samples from cells in culture, including the outliers. Using only PEL-derived data for PCA afforded us the resolution to identify differences among individual PEL isolates. Ten of 13 PEL cell lines clustered tightly together (data not shown), which reaffirmed the initial, phenotype-based classification of PEL. We also observed 3 unique samples: BCLM and VG1, in addition to the previously noted JSC1.

On analyzing the CNV markers in detail, we identified discrete regions of amplifications and deletions on each chromosome, many of which were shared in > 50% of the samples. Supplemental Figure 1 (available on the *Blood* Web site; see the Supplemental

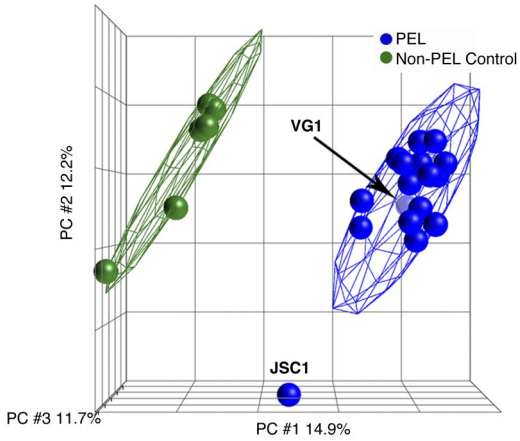

Figure 1. PCA of PEL. PCA shows the presence of 2 distinct clusters formed by endothelial cells in green and all the 17 (excluding JSC1) PEL cells in blue, irrespective of whether they were from culture or xenograft. The x-, y-, and z-axes represent PC1, PC2, and PC3, respectively, accounting for 14.9%, 12.2%, and 11.7% of variability in the data.

Materials link at the top of the online article) shows the heat map representation of CNV for PEL cell lines. The top panel shows the EBV-positive and the bottom panel EBV-negative PEL cell lines. Chromosomes 7, 8, 12, and the q-arm of chromosome 1 harbored most of the amplifications.

We verified the CNV data with the use of G-band karyotyping of a subset of the samples: BC1, BC3, BCBL1, and BCP1. These samples were chosen to include PELs with or without EBV coinfection and mutation in the p53 gene (as listed in Table 1). On comparing our CNV heat map (supplemental Figure 1) with our karyotyping data (supplemental Figure 2), we see a tight correlation in detecting gross chromosomal aberrations between the 2 methods.

All of the cell lines showed trisomy of chromosome 7 with a subset showing trisomy of chromosome 12 (BC1 and BCP1) and amplification of 1q (BC1 and BCP1), in agreement with previous cytogenetic studies on these cell lines.[6,33] In addition, we noticed amplifications and deletions throughout the genome (supplemental Figure 2) and varying among individual cell lines. When we compared this data and previous reports,[5,6,33-35] we note the variability of karyotype aberrations. We further note the power of array-based CGH over traditional karyotyping to detect smaller changes that might be more tightly associated with the PEL phenotype than gross variation in karyotype.

The 946 000 CNV-specific probes that are contained in the Affymetrix 6.0 array allowed us, for the first time, to define the genomic signature exhibited by PEL cells at a single gene resolution. Table 2 shows the individual genes with CNV in 12 of 13 PEL cell lines. This represents our most stringent cutoff. Two of these, *WWOX* and *FHIT*, represent common fragile site (CFS) genes. The glutamate receptor ionotrophic, delta 2 (*GRID2*) gene that was deleted exclusively from the EBV-negative PEL cell lines (listed in Table 3) is also classified as a CFS gene. CFSs are regions of the genome particularly susceptible to breaks in metaphase chromosomes. These regions are evolutionarily conserved and tend to encode for genes involved in tumor suppression, replicative stress, and DNA damage repair.[36] *FHIT*, *WWOX*, and *GRID2* map to the CFS FRA3D, FRA16D, and FRA4G on chromosomes 3 (p-arm), 16 (q-arm), and 4 (q-arm), respectively.[37-39] Figure 2 shows the detailed distribution of markers around these 3 sites in our PEL samples as well as non-PEL controls. Figure 2A and C represent the PEL samples that were hybridized to the Affymetrix 6.0 and the second, independent, Affymetrix 500K array, respectively. We note that in both cases, irrespective of the density of the markers used, we observe a localized loss of CFS genes in an otherwise normal region of the chromosome. For comparison, the q-arm of chromosome 4 in the same panels (Figure 2A,C) is an example of large-scale chromosomal amplification. These large-scale rearrangements were present in >1 PEL cell line, but by no means in all cell lines. The control samples in which these

Table 2. Genes deregulated in majority of PEL cell lines

Gene ID	Gene name	Location	Amplification	Deletion	EBV dependent
DERL1	DER-1 like domain family, member 1	8q24.13	AP2, AP5, BC1, BC2, BC3, BCBL, BCLM, BCP1, HHB2, JSC1, TY1, VG1	None	No
ETV1	ETS translocation variant 1	7p21.3	AP5, BC1, BC2, BC3, BC5, BCBL, BCLM, BCP1, HHB2, JSC1, TY1, VG1	None	No
RASA4	RAS p21 protein activator 4	7q22	AP2, AP5, BC1, BC3, BC5, BCBL, BCLM, BCP1, HHB2, JSC1, TY1, VG1	None	No
TPK1	Thiamin pyrophosphokinase 1	7q34	AP2, AP5, BC1, BC3, BC5, BCBL, BCLM, BCP1, HHB2, JSC1, TY1, VG1	None	No
TRIM56	TRIpartite motif-containing 56	7q22.1	AP2, AP5, BC1, BC3, BC5, BCBL, BCLM, BCP1, HHB2, JSC1, TY1, VG1	None	No
VPS41	Vacuolar protein sorting 41 homolog	7p14	AP2, AP5, BC1, BC3, BC5, BCBL, BCLM, BCP1, HHB2, JSC1, TY1, VG1	None	No
*WWOX**	WW-domain containing oxidoreductase	16q23.3	None	AP5, BC1, BC2, BC3, BC5, BCBL, BCLM, BCP1, HHB2, JSC1, TY1, VG1	No
*FHIT**	Fragile histidine triad	3p14.2	None	AP2, AP5, BC1, BC2, BC3, BC5, BCBL, BCLM, BCP1, TY1, VG1	No
*GRID2**	Glutamate receptor, ionotropic, δ 2	4q22.1	None	BC3, BCBL, BCLM, TY1, VG1	Yes

*Common fragile site genes.

Table 3. Genes altered only in EBV-negative PEL

Gene ID	Gene name	Location	Category	Amplification	Deletion	Unchanged
ACSBG2	Acyl-CoA synthetase bubblegum family member 2	19p13.3	Metabolism	BC3, BCBL, BCLM, BCP1, HHB2, TY1		VG1
FUT3	CD174; Fucosyltransferase 3	19p13.3	Metabolism	BC3, BCBL, BCLM, BCP1, HHB2, TY1		VG1
HLA-DRB5	MHC-II, DR-β-5	6p21.3	MHC	BCBL, BCLM, BCP1, TY1, VG1		BC3, HHB2
IKBKB	IκB kinase β	8p11.2	Cell signaling	BC3, BCBL, BCLM, BCP1, TY1		HHB2, VG1
ITPR1	Inositol-1,4,5-triphosphate receptor, type 1	3p26.1	Cell signaling	BCBL, BCLM, BCP1, TY1, VG1		BC3, HHB2
RAF1	v-Raf murine leukemia homolog 1	3p25	Oncogene	BCBL, BCLM, BCP1, TY1, VG1		BC3, HHB2
RFX2	Regulatory factor X, 2	19p13.3	Transcription	BC3, BCBL, BCLM, BCP1, HHB2		TY1, VG1
ARAP2	Arf and RhoGAP adaptor protein 2	4p14	Cytoskeleton		BC3, BCBL, BCP1, HHB2, TY1	BCLM, VG1
BRCA2	Breast cancer 2, early onset	13q12.3	Tumor suppressor		BC3, BCBL, BCLM, HHB2, TY1	BCP1, VG1
CADM2	Cell adhesion molecule 2	3p11.1	Cell adhesion		BC3, BCBL, BCP1, HHB2, TY1	BCLM, VG1
CDH9	Cadherin 9, type 2	5p14.1	Cell adhesion	HHB2	BC3, BCBL, BCLM, BCP1, TY1	VG1
CDYL	Chromodomain protein, Y-like	6p25.1	Transcription	VG1	BCBL, BCLM, BCP1, HHB2, TY1	BC3
CHD1	Chromodomain helicase DNA binding protein 1	5q21.1	Transcription	HHB2	BCBL, BCLM, BCP1, TY1, VG1	BC3
EPHA3	Ephrin receptor A3	3p11.2	Development		BC3, BCBL, BCLM, BCP1, TY1	HHB2, VG1
EPHA5	Ephrin receptor A5	4q13.1	Development	VG1	BC3, BCBL, BCLM, BCP1, HHB2, TY1	
EDIL3	EGF-like repeats and discoidin-I like domain 3	5q14.3	Cell adhesion	HHB2	BC3, BCBL, BCLM, BCP1, TY1	VG1
GRID2	Glutamate receptor, ionotropic, δ 2	4q22.1	Development		BC3, BCBL, BCLM, TY1, VG1	BCP1, HHB2
HBS1L	Hsp70 subfamily B suppressor 1-like protein	6q23.3	Development		BCBL, BCLM, BCP1, HHB2, TY1	BC3, VG1
LRFN5	Leucine rich repeat and fibronectin type III domain containing 5	14q21.1	Cell adhesion		BC3, BCBL, BCLM, BCP1, TY1	HHB2, VG1
MEF2C	Myocyte enhancer factor 2	5q14.3	Transcription	HHB2	BC3, BCBL, BCP1, TY1, VG1	BCLM
PCDH9	Protocadherin 9	13q21.32	Cell adhesion		BC3, BCBL, BCLM, BCP1, TY1	HHB2, VG1
RREB1	Ras-responsive element binding protein 1	6p24.3	Transcription	BC3, VG1	BCBL, BCP1, HHB2, TY1	BCLM
ZEB1	Zinc finger E-box binding homeobox 1	10p11.2	Transcription		BC3, BCBL, BCLM, BCP1, HHB2	TY1, VG1

markers were assessed in non-PEL tumor samples are shown in Figure 2B and D. Figure 2B contains 6 tumor samples of non–B-cell origin (both KSHV positive and negative) hybridized to the 6.0 SNP array, and Figure 2D shows 5 non-PEL lymphoma samples hybridized to the 500K SNP array. Neither sets of controls show loss of *FHIT*, *WWOX*, or *GRID2* genes. This shows that the partial or complete loss of *FHIT* (11 of 13, 85% of PEL cell lines), *WWOX* (12 of 13, 92% of PEL cell lines), and *GRID2* (5 of 7, 71% of EBV-negative PEL cell lines) in an otherwise normal chromosomal setting is particular to PEL. We also investigated other CFS regions such as retinoid-related orphan receptor α (*RORA*) on chromosome 15 and Parkinson disease 2 (*PARK2*) on chromosome 6. There was no amplification or deletion detected in these regions (data not shown). This further supported our conclusion that deletion of *FHIT*, *WWOX*, and *GRID2* cannot be attributed to the fragility of these regions but represent selected mutations characteristic of PEL cell lines.

Table 2 also contains genes that were significantly amplified in 12 of 13 (92%) PEL cell lines based on the Affymetrix arrays. These are DER-like family member 1 (*DERL1*), ETS translocation variant 1 (*ETV1*), RAS p21 activator protein 4 (*RASA4*), thiamin pyrophospho-kinase 1 (*TPK1*), tripartite motif containing 56 (*TRIM56*), and vacuolar protein sorting-41, homolog (*VPS41*). Other genes were deleted or amplified in a smaller fraction of samples. Although these alterations may have biological relevance alone or in combination, the significance of these candidate alterations needs to be established in a larger number of cases.

With the use of qPCR we verified a subset of our CNV data: DERL1, as an example of gene amplification, and the 3 fragile site tumor suppressor genes. Figure 3 shows a histogram of the copy number of samples relative to the normal diploid copy number per genome (ddCT) for PEL (n = 13) and non-PEL (n = 11) tumor cell lines. Where normal cells have a ddCT of 0, amplifications and deletions are represented by positive and negative ddCTs, respectively. Note that in this representation the results of individual cell lines are stacked to give a measure of the degree as well as frequency of the genomic aberration.[40] Figure 3A represents the *DERL1* locus, which was shown to be amplified in PEL by CGH, and we subsequently confirmed this by PCR, as evidenced by a positive ddCT. The same gene was also amplified in a subset of non-PEL tumor cell lines (those with no amplification have a ddCT of 0 and thus do not contribute to the signal). Figure 3B-D shows the results for *FHIT*, *GRID2*, and *WWOX*, respectively. Compared with normal human genomic DNA, PEL cell lines show losses of *WWOX*, *FHIT*, and *GRID2*. These qPCR data confirmed independently our array analysis. *FHIT* and *GRID2* were also deleted in some non-PEL tumor cell lines, as expected for a fragile site. *WWOX*, however, was exclusively deleted in PEL and not in the other tumor samples ($P \leq .005$ by Wilcoxon nonparametric test). If anything, *WWOX* seemed increased in some non-PEL tumor cells. Again, this would be expected for a random set of tumors, all of which do show some degree of gross genome alterations. It is important to note the scale of the genomic changes, which does not

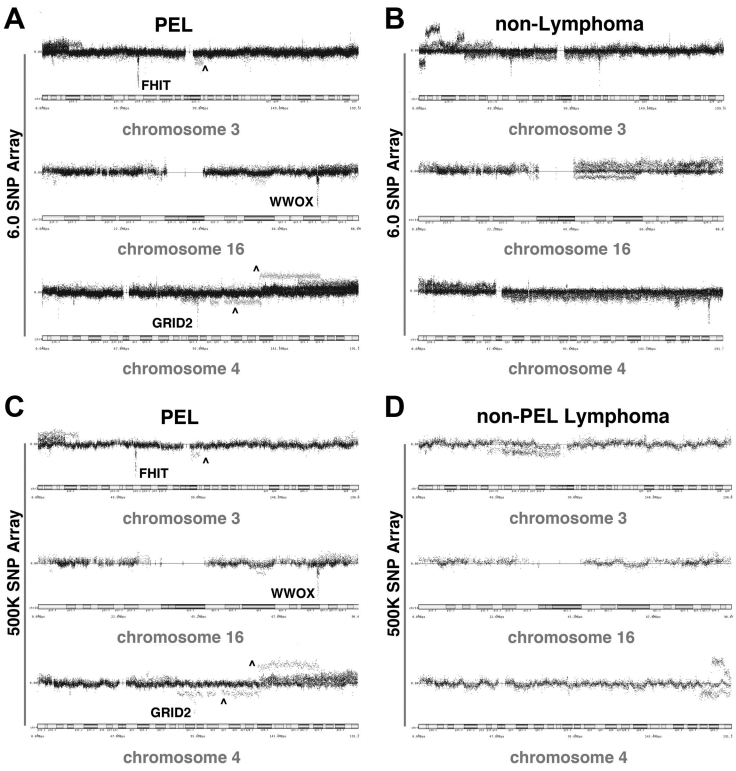

Figure 2. CFS tumor suppressor genes *FHIT*, *WWOX*, and *GRID* dot plot in PEL. Dot plot representation of markers distributed along the chromosome. (A,C) The loss of FHIT, WWOX, and GRID2 from chromosomes 3, 16, and 4, both in the 6.0 and 500K SNP array are shown. The markers (from each of the 13 PELs) are represented by black dots on a $\log_2$ scale (amplification denoted by dots above and deletion by dots below the normal 0 line) with the cytoband at the base of plot. The dots identified by ^ represent alterations that only occurred in 1 of 13 PELs and were thus considered exceptions. (B,D) Data represent 6 nonlymphoma tumor samples and 5 non-PEL lymphoma controls, respectively.

exceed 2-fold for individual amplifications, consistent with large-scale CNV. By contrast, the KSHV probe (Figure 3E) exemplifies the signal differences because of large copy number increases (as denoted by the difference in scale), because KSHV is present in ~ 50 copies in PEL, but was present in only 5 of our 11 non PEL-tumor lines and here at 1 or < 1 copy per cell.

CNV, not LOH, distinguishes EBV-positive from EBV-negative PEL

A tally of the CNV markers showed a significantly ($P \leq .05$ by *t* test) greater number of amplifications in the EBV-negative group than in the EBV-positive cell lines (Figure 4A). The data for deletions mirror the trend; EBV-negative cells harbor more deletions than the EBV-positive group (Figure 4B), although the level of significance was lower ($P \leq .1$ by *t* test). Using PCA, we demonstrated the presence of 2 distinct subclusters within PEL cell lines (Figure 4C). These 2 distinct clusters correlate with EBV infection status, JSC1 and VG1 being the outliers (analogous to our initial PCA).

We further mapped the CNV markers to the RefSeq database[19] to identify specific genes. Table 3 shows 23 genes that were most significantly altered in EBV-negative PEL cell lines. We used false-discovery rate that was based on adjustment for multiple comparisons and defined q-values ≤ 0.01 as cutoff. We annotated this list with the use of GeneCards database v3.0.[41] On the basis of their known functions, the genes were classified into (1) transcriptional (*CDYL*, *CHD1*, *MEF2C*, *RFX2*, *RREB1*, *ZEB1*), (2) developmental (*EPHA-3*, *-5*, *GRID2*, *HBS1L*), (3) metabolic (*ACSBG2*, *FUT3*), (4) cell signaling (*IKBKB*, *ITPR1*), and (5) cell adhesion (*CADM2*, *CDH9*, *EDIL3*, *LRFN5*, *PCDH9*) molecules. The oncogene *RAF1*, tumor suppressor *BRCA2*, cytoskeletal regulator *ARAP2*, and MHC receptor *HLA-DRB5* were assigned their own categories.

In addition to CNV, the Affymetrix 6.0 SNP markers allowed us to interrogate LOH in PEL for the first time. LOH is indicative of allelic imbalance and can be used to assess overall genomic integrity.[42] Unstable genomes harbor a greater extent of LOH compared with those that are genetically stable. The presence of allelic imbalance (LOH) did not correlate with EBV infection status in the PEL cell lines. Both EBV-positive and EBV-negative groups harbor the same degree of copy neutral LOH (indicative of

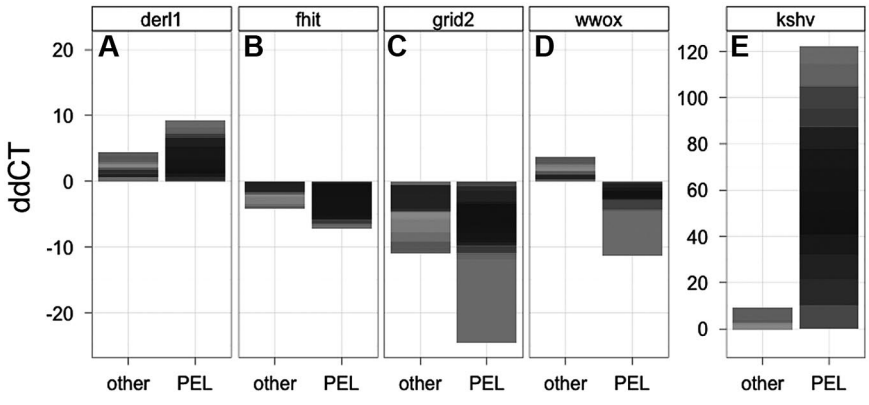

Figure 3. qPCR verification of CFS tumor suppressor gene loss in PEL. (A-E) The qPCR results for DERL1, FHIT, GRID2, WWOX, and KSHV, respectively, are shown. Shown is the stacked relative level (ddCT) for each gene on the vertical axis and the 2 classes of 13 non-PEL (other) and 13 PEL cell lines on the horizontal axis. The contribution of individual cell lines is indicated by the gray level. Because amplifications and deletions result in only a 2-fold change in signal in the case of cellular genes (and ~ 50-fold for KSHV because there are ~ 50 copies of the KSHV genome in each PEL cell) the stacked representation integrates both the degree of change as well as the number of cell lines that contribute to the signal in each group (a similar metric was previously validated).[39]

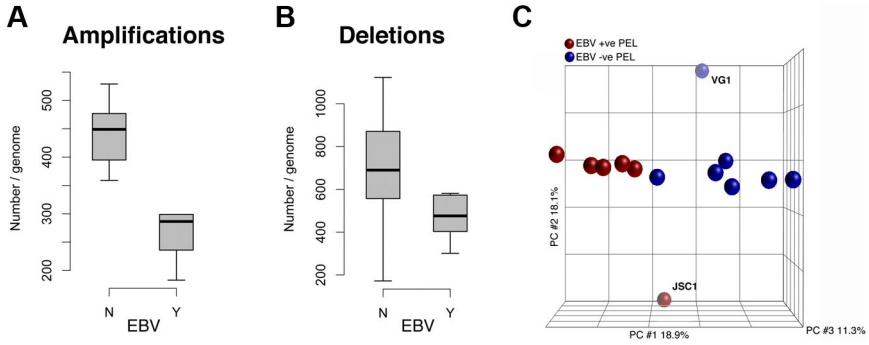

Figure 4. Quantification of CNV in PEL, separated by EBV status. (A) There are significantly more amplifications in EBV-negative PELs than in EBV-positive PELs. (B) Although there is increased deletion of markers in the EBV-negative population, there difference is less conclusive. (C) PCA shows that PEL cells in culture form 2 distinct groups correlative with their EBV infection status: blue indicates EBV(−) and brown EBV(+) samples. The x-, y-, and z-axes represent PC1, PC2, and PC3, respectively, accounting for 18.9%, 18.1%, and 11.3% of variability in the data.

uniparental disomy) and heterozygous gains or losses (data not shown). In summary, CNV (amplifications/deletions) but not LOH separate EBV-positive from EBV-negative PEL cell lines.

Discussion

In this study we defined the genomic signature of PEL cell lines at the individual gene level with the use of Affymetrix SNP6.0 array–based CGH. Most of the genetic changes corresponded to broad amplifications of regions of chromosome 7, 8, 12 and q-arm of 1. This first high-resolution data extend earlier studies that have reported similar observations in a single PEL or in a smaller collection of PEL cell lines with the use of first-generation BAC-mid–based CGH arrays.[5,6,33-35] This study for the first time associates 3 fragile site tumor suppressor genes, *FHIT*, *WWOX*, and *GRID2*, with PEL cell lines. PEL cell lines maintained the same genomic signatures whether grown in culture or as xenograft in a SCID mouse, which is consistent with the monoclonal origin of PEL. The presence of EBV, in addition to KSHV, was associated with decreased gross genomic rearrangements in PEL cell lines.

This first high-resolution CGH analysis of PEL cell lines allowed us to identify individual genes that were deleted or amplified. The 2 most prominent deletions were the fragile site genes *WWOX* and *FHIT*. Similar SNP-based array studies have been performed for Burkitt lymphoma (BL) with the use of lower resolution arrays.[43,44] The 2 studies reported distinct sets of aberrations. Where Scholtysik et al[44] commented on the imbalances affecting the *MYC* locus, Toujani et al[43] found loss of *FHIT* to be one of the most common losses in BL primary tumors as well as cell lines. *WWOX* and *FHIT* have been classified as tumor suppressor genes in multiple cancers, including DLBCL.[37,38,45,46] Transgenic mice that lack *FHIT* or *WWOX* are more prone to developing tumors, especially those of the lymphoid origin.[47,48] Reintroduction of the respective tumor suppressor genes, ectopically or by gene therapy, restores nontumor properties in the mice.[49,50] It can be speculated that in PEL, as in other DLBCLs, a loss of function of these genes promotes tumorigenesis. One might even hypothesize that the reintroduction of *FHIT* or *WWOX* may be developed into a gene transfer–based therapy for PEL.

We detected 6 nonfragile site genes that were amplified in most of the PEL cell lines. *DERL1* and *ETV1* have previously been associated with viral and nonviral cancers.[51,52] *DERL1* protects cells from endoplasmic reticulum (ER) stress–induced apoptosis and is overexpressed in breast cancer.[52] Multiple reports have shown associations between solid tumors and *ETV1*, and alteration in *ETV1* is a prognostic marker in tumor progression.[51] Yet the specific biochemical function of *ETV1* remains to be elucidated. The remaining high-significance amplifications include Ras-p21 activator protein 4 (*RASA4*), tyrosine protein kinase 1 (*TPK1*), tripartite-motif containing 56 (*TRIM56*), and vacuolar protein sorting 41 homolog (*VSP41*). These are involved in cell signaling, metabolism, and protein maturation. This study, for the first time, suggests that these genes may be involved in cancer.

PEL is believed to be a monoclonal expansion of a post-GC B cell.[53,54] Immunophenotypic analysis suggests that PELs comprise a subset of plasma cells. Normally, naive B cells entering the GC undergo B-cell receptor (BCR)–mediated differentiation/activation to form memory and plasma cells. Those that cannot be stimulated because of lack of BCR or crippling mutations are eliminated via Fas-mediated apoptosis. However, in PEL as well as EBV-positive posttransplant-associated lymphomas, a subset of these cells escapes apoptosis and ultimately develops into lymphoma. By some account this escaping population of cells lacking functional BCR is particularly susceptible to EBV infection; EBV infection not only protects them from GC-mediated apoptosis but also contributes to proliferation.[55]

Mack and Sugden[11] reported that EBV is essential for sustained proliferation of some EBV-positive PELs in culture, but EBV-negative PEL cell lines exhibit similar sustained proliferation in culture and tumor-forming potential in mice.[13] This study for the first time found a PEL genotype that is associated with EBV infection: EBV-negative PEL cell lines harbor significantly more gross genomic alterations than EBV-positive PEL cell lines. EBV appears to facilitate host chromosomal genomic stability in PEL cells. This phenotype is consistent with EBV-transformed lymphoblastoid cell lines that retain a normal karyotype indefinitely.[56] Vaghefi et al[57] suggested that for KSHV-negative AIDS lymphomas an inverse correlation exists between EBV infection and the number of chromosomal aberrations. At this point it is unclear whether this is because of a direct stabilizing effect of EBV latent genes or whether the expression of EBV latent genes relieves selective pressure for additional genomic alterations in host oncogene or tumor suppressor gene loci by modulating growth-promoting pathways posttranslationally (which EBV-negative PEL would need to be selected by genomic alterations). Alternatively, the possibility exists that the genomic aberration is a result of EBV-negative PEL cells having traversed the GC[51] and EBV-positive PEL not.

The contribution of EBV to PEL development has remained a matter of debate; EBV-positive and EBV-negative PEL cell lines exhibit the same tumor characteristics in mouse models and in the clinic. Here, we can speculate on a couple different scenarios of PEL tumor progression. One being, a "sequential" scenario, whereby KSHV-infected naive B cells entering the GC are infected with EBV that drives them through the maturation/differentiation process and contributes to their proliferative advantage. Some of the EBV-infected B cells subsequently acquire the PEL-defining

FHIT and *WWOX* gene mutations. As these tumor cells continue to evolve, some of them may lose the EBV episome but acquire additional compensatory genetic mutations, by a yet undefined mechanism. This would give rise to EBV-negative PEL, in other cases EBV is never lost. Alternatively, KSHV-infected naive B cells traversing through the GC remain EBV negative but acquire *FHIT* and *WWOX* mutations. Subsequently, these mutant cells are either infected with EBV or acquire additional genetic mutations to form fulminant PEL. This leads to 2 alternative, or "parallel," tumor development pathways. Such a scenario mirrors the situation in EBV-positive versus EBV-negative BL. Unfortunately, because PEL causes such rapid mortality, no longitudinal samples exist to clinically verify this model.

In Table 3, we also noted individual genes that were correlated with EBV status. A significant number of those were involved with cell adhesion. For known tumor genes, we note amplification of *RAF1* or *c-RAF* and deletion of the tumor suppressor gene breast cancer gene 2, *BRAC2*, in EBV-negative PEL. *c-RAF* is the cellular homolog of the murine leukemia viral oncogene, *v-RAF-1*, a serine/threonine-specific protein kinase involved in the MAPK-ERK pathway, and *BRCA2* is associated with DNA damage repair, specifically, double strand breaks and homologous recombination.

Other interesting genes that were significantly amplified in EBV-negative PEL include *IKBKB*, IKB kinase-β, a key activator of NFκB, and *ITPR1*, inositol-1,4,5-triphosphate receptor 1. NFκB has a known role in PEL tumorigenesis. It is modulated by the KSHV homolog of the cellular FLICE inhibitory protein (vFLIP)[52,58] as well as KSHV K15.[59] Of note, the EBV latency membrane protein 1 (LMP-1) can also activate NFκB.[60] Thus, it seems consistent with the biology of EBV that *IKBKB*, a cellular activator of NFκB, was amplified in 5 of 7 EBV-negative cells. *ITPR1* is involved in regulating calcium homeostasis in the ER, inducing Ca^{2+} release into the cytosol. Normal B cells undergoing activation and blastic transformation show elevated levels of cytosolic Ca^{2+}.[61] It has been shown by Dellis et al[62] that EBV LMP-1 can down-regulate ER-associated enzymes to increase levels of cytosolic Ca^{2+} and promote cellular transformation. Therefore, it can be hypothesized that amplification of *ITPR1* in EBV-negative PEL compensates for the absence of EBV-LMP1 to drive B-cell transformation.

Finally, one of the genes deleted exclusively in EBV-negative PEL cell lines, *GRID2*, is also a fragile site gene. Deletion of *GRID2* was observed in 5 of 7 EBV-negative PEL cell lines, whereas it remained unaltered in EBV-positive PEL cell lines. This further speaks to the instability of the host genome in the absence of EBV in PEL cell lines. *GRID2* is noted for its role in neurologic development.[36] Ours is the second report suggesting a role for *GRID2* in tumorigenesis.[63]

In summary, this represents the first high-resolution CGH analysis of PEL cell lines. We find evidence of genomic instability, which was greater in EBV-negative PEL cell lines. We verify that the PEL-associated genomic signature maps mainly to amplifications in chromosome 7, 8, and 12 and the q-arm of 1. We report the first association of deletion of the fragile site tumor suppressor genes *FHIT* and *WWOX* with PEL cell lines and *GRID2* with EBV-negative PEL cell lines.

Acknowledgments

The authors thank K. L. Richards for critical reading of the manuscript.

This work was supported in part by the National Institutes of Health grants DE018304, CA019014, CA163217, CA096500, and DE018281; the Centers for AIDS research (CfAR); the AIDS malignancy consortium (grant CA121947); the University Cancer Research Fund (UCRF); and the Leukemia & Lymphoma Society of America (grant R6169-10). B.D. is a scholar of the Leukemia & Lymphoma Society and a Burrows Welcome trust investigator.

Authorship

Contribution: D.R. designed and conducted experiments, analyzed data, and wrote manuscript; S.-H.S. conducted experiments; B.D. designed experiments and analyzed data; and D.P.D. designed experiments, analyzed data, and wrote manuscript.

Conflict-of-interest disclosure: The authors declare no competing financial interests.

Correspondence: Dirk P. Dittmer, Curriculum in Genetics and Molecular Biology and Department of Microbiology and Immunology, UNC Lineberger Comprehensive Cancer Center, UNC Center for AIDS Research, University of North Carolina at Chapel Hill, CB# 7290, Mary Ellen Jones Bldg, Chapel Hill, NC 27599-7290; e-mail: ddittmer@med.unc.edu.

References

1. Chadburn A, Hyjek E, Mathew S, Cesarman E, Said J, Knowles DM. KSHV-positive solid lymphomas represent an extra-cavitary variant of primary effusion lymphoma. *Am J Surg Pathol.* 2004;28(11):1401-1416.
2. Nador RG, Cesarman E, Chadburn A, et al. Primary effusion lymphoma: a distinct clinicopathologic entity associated with the Kaposi's sarcoma-associated herpes virus. *Blood.* 1996;88(2):645-656.
3. Klein U, Gloghini A, Gaidano G, et al. Gene expression profile analysis of AIDS-related primary effusion lymphoma (PEL) suggests a plasmablastic derivation and identifies PEL-specific transcripts. *Blood.* 2003;101(10):4115-4121.
4. O'Hara AJ, Vahrson W, Dittmer DP. Gene alteration and precursor and mature microRNA transcription changes contribute to the miRNA signature of primary effusion lymphoma. *Blood.* 2008; 111(4):2347-2353.
5. Ohshima K, Ishiguro M, Yamasaki S, et al. Chromosomal and comparative genomic analyses of HHV-8-negative primary effusion lymphoma in five HIV-negative Japanese patients. *Leuk Lymphoma.* 2002;43(3):595-601.
6. Nair P, Pan H, Stallings RL, Gao SJ. Recurrent genomic imbalances in primary effusion lymphomas. *Cancer Genet Cytogenet.* 2006;171(2):119-121.
7. Chang Y, Cesarman E, Pessin MS, et al. Identification of herpesvirus-like DNA sequences in AIDS-associated Kaposi's sarcoma. *Science.* 1994;266(5192):1865-1869.
8. Soulier J, Grollet L, Oksenhendler E, et al. Kaposi's sarcoma-associated herpesvirus-like DNA sequences in multicentric Castleman's disease. *Blood.* 1995;86(4):1276-1280.
9. Fakhari FD, Dittmer DP. Charting latency transcripts in Kaposi's sarcoma-associated herpesvirus by whole-genome real-time quantitative PCR. *J Virol.* 2002;76(12):6213-6223.
10. Fan W, Bubman D, Chadburn A, Harrington WJ Jr, Cesarman E, Knowles DM. Distinct subsets of primary effusion lymphoma can be identified based on their cellular gene expression profile and viral association. *J Virol.* 2005;79(2):1244-1251.
11. Mack AA, Sugden B. EBV is necessary for proliferation of dually infected primary effusion lymphoma cells. *Cancer Res.* 2008;68(17):6963-6968.
12. Staudt MR, Kanan Y, Jeong JH, Papin JF, Hines-Boykin R, Dittmer DP. The tumor microenvironment controls primary effusion lymphoma growth in vivo. *Cancer Res.* 2004;64(14):4790-4799.
13. Sin SH, Roy D, Wang L, et al. Rapamycin is efficacious against primary effusion lymphoma (PEL) cell lines in vivo by inhibiting autocrine signaling. *Blood.* 2007;109(5):2165-2173.
14. Rowley JD. Letter: a new consistent chromosomal abnormality in chronic myelogenous leukaemia identified by quinacrine fluorescence and Giemsa staining. *Nature.* 1973;243(5405):290-293.
15. Petre CE, Sin SH, Dittmer DP. Functional p53

signaling in Kaposi's sarcoma-associated herpesvirus lymphomas: implications for therapy. *J Virol.* 2007;81(4):1912-1922.

16. Bubman D, Guasparri I, Cesarman E. Deregulation of c-Myc in primary effusion lymphoma by Kaposi's sarcoma herpesvirus latency-associated nuclear antigen. *Oncogene.* 2007;26(34):4979-4986.
17. Gaidano G, Capello D, Cilia AM, et al. Genetic characterization of HHV-8/KSHV-positive primary effusion lymphoma reveals frequent mutations of BCL6: implications for disease pathogenesis and histogenesis. *Genes Chromosomes Cancer.* 1999;24(1):16-23.
18. Boulanger E, Marchio A, Hong SS, Pineau P. Mutational analysis of TP53, PTEN, PIK3CA and CTNNB1/beta-catenin genes in human herpesvirus 8-associated primary effusion lymphoma. *Haematologica.* 2009;94(8):1170-1174.
19. National Center for Biotechnology Information. Reference Sequence database. http://www.ncbi.nlm.nih.gov/RefSeq/. Accessed March 2010.
20. D'Haene B, Vandesompele J, Hellemans J. Accurate and objective copy number profiling using real-time quantitative PCR. *Methods.* 2010;50(4):262-270.
21. Carbone A, Cilia AM, Gloghini A, et al. Establishment of HHV-8-positive and HHV-8-negative lymphoma cell lines from primary lymphomatous effusions. *Int J Cancer.* 1997;73(4):562-569.
22. Carbone A, Cilia AM, Gloghini A, et al. Establishment and characterization of EBV-positive and EBV-negative primary effusion lymphoma cell lines harbouring human herpesvirus type-8. *Br J Haematol.* 1998;102(4):1081-1089.
23. Cesarman E, Moore PS, Rao PH, Inghirami G, Knowles DM, Chang Y. In vitro establishment and characterization of two acquired immunodeficiency syndrome-related lymphoma cell lines (BC-1 and BC-2) containing Kaposi's sarcoma-associated herpesvirus-like (KSHV) DNA sequences. *Blood.* 1995;86(7):2708-2714.
24. Arvanitakis L, Mesri EA, Nador RG, et al. Establishment and characterization of a primary effusion (body cavity-based) lymphoma cell line (BC-3) harboring Kaposi's sarcoma-associated herpesvirus (KSHV/HHV-8) in the absence of Epstein-Barr virus. *Blood.* 1996;88(7):2648-2654.
25. Guasparri I, Keller SA, Cesarman E. KSHV vFLIP is essential for the survival of infected lymphoma cells. *J Exp Med.* 2004;199(7):993-1003.
26. Komanduri KV, Luce JA, McGrath MS, Herndier BG, Ng VL. The natural history and molecular heterogeneity of HIV-associated primary malignant lymphomatous effusions. *J Acquir Immune Defic Syndr Hum Retrovirol.* 1996;13(3):215-226.
27. Ghosh SK, Wood C, Boise LH, et al. Potentiation of TRAIL-induced apoptosis in primary effusion lymphoma through azidothymidine-mediated inhibition of NF-kappa B. *Blood.* 2003;101(6):2321-2327.
28. Boshoff C, Gao SJ, Healy LE, et al. Establishing a KSHV+ cell line (BCP-1) from peripheral blood and characterizing its growth in Nod/SCID mice. *Blood.* 1998;91(5):1671-1679.
29. Gradoville L, Gerlach J, Grogan E, et al. Kaposi's sarcoma-associated herpesvirus open reading frame 50/Rta protein activates the entire viral lytic cycle in the HH-B2 primary effusion lymphoma cell line. *J Virol.* 2000;74(13):6207-6212.
30. Cannon JS, Ciufo D, Hawkins AL, et al. A new primary effusion lymphoma-derived cell line yields a highly infectious Kaposi's sarcoma herpesvirus-containing supernatant. *J Virol.* 2000;74(21):10187-10193.
31. Katano H, Hoshino Y, Morishita Y, et al. Establishing and characterizing a CD30-positive cell line harboring HHV-8 from a primary effusion lymphoma. *J Med Virol.* 1999;58(4):394-401.
32. Brander C, Suscovich T, Lee Y, et al. Impaired CTL recognition of cells latently infected with Kaposi's sarcoma-associated herpes virus. *J Immunol.* 2000;165(4):2077-2083.
33. Gaidano G, Capello D, Fassone L, et al. Molecular characterization of HHV-8 positive primary effusion lymphoma reveals pathogenetic and histogenetic features of the disease. *J Clin Virol.* 2000;16(3):215-224.
34. Mullaney BP, Ng VL, Herndier BG, McGrath MS, Pallavicini MG. Comparative genomic analyses of primary effusion lymphoma. *Arch Pathol Lab Med.* 2000;124(6):824-826.
35. Boulanger E, Agbalika F, Maarek O, et al. A clinical, molecular and cytogenetic study of 12 cases of human herpesvirus 8 associated primary effusion lymphoma in HIV-infected patients. *Hematol J.* 2001;2(3):172-179.
36. Durkin SG, Glover TW. Chromosome fragile sites. *Annu Rev Genet.* 2007;41:169-192.
37. Ohta M, Inoue H, Cotticelli MG, et al. The FHIT gene, spanning the chromosome 3p14.2 fragile site and renal carcinoma-associated t(3;8) breakpoint, is abnormal in digestive tract cancers. *Cell.* 1996;84(4):587-597.
38. Bednarek AK, Laflin KJ, Daniel RL, Liao Q, Hawkins KA, Aldaz CM. WWOX, a novel WW domain-containing protein mapping to human chromosome 16q23.3-24.1, a region frequently affected in breast cancer. *Cancer Res.* 2000;60(8):2140-2145.
39. Rozier L, El-Achkar E, Apiou F, Debatisse M. Characterization of a conserved aphidicolin-sensitive common fragile site at human 4q22 and mouse 6C1: possible association with an inherited disease and cancer. *Oncogene.* 2004;23(41):6872-6880.
40. Beroukhim R, Getz G, Nghiemphu L, et al. Assessing the significance of chromosomal aberrations in cancer: methodology and application to glioma. *Proc Natl Acad Sci U S A.* 2007;104(50):20007-20012.
41. Weizmann Institute of Science. GeneCards. http://www.genecards.org. Accessed March 2010.
42. Kawai H, Suda T, Aoyagi Y, et al. Quantitative evaluation of genomic instability as a possible predictor for development of hepatocellular carcinoma: comparison of loss of heterozygosity and replication error. *Hepatology.* 2000;31(6):1246-1250.
43. Toujani S, Dessen P, Ithzar N, et al. High resolution genome-wide analysis of chromosomal alterations in Burkitt's lymphoma. *PLoS ONE.* 2009;4(9):e7089.
44. Scholtysik R, Kreuz M, Klapper W, et al. Detection of genomic aberrations in molecularly defined Burkitt's lymphoma by array-based, high resolution, single nucleotide polymorphism analysis. *Haematologica.* 2010;95(12):2047-2055.
45. Deffenbacher KE, Iqbal J, Liu Z, Fu K, Chan WC. Recurrent chromosomal alterations in molecularly classified AIDS-related lymphomas: an integrated analysis of DNA copy number and gene expression. *J Acquir Immune Defic Syndr.* 2010;54(1):18-26.
46. Kameoka Y, Tagawa H, Tsuzuki S, et al. Contig array CGH at 3p14.2 points to the FRA3B/FHIT common fragile region as the target gene in diffuse large B-cell lymphoma. *Oncogene.* 2004;23(56):9148-9154.
47. Aqeilan RI, Trapasso F, Hussain S, et al. Targeted deletion of Wwox reveals a tumor suppressor function. *Proc Natl Acad Sci U S A.* 2007;104(10):3949-3954.
48. Ludes-Meyers JH, Kil H, Nunez MI, et al. WWOX hypomorphic mice display a higher incidence of B-cell lymphomas and develop testicular atrophy. *Genes Chromosomes Cancer.* 2007;46(12):1129-1136.
49. Dumon KR, Ishii H, Fong LY, et al. FHIT gene therapy prevents tumor development in Fhit-deficient mice. *Proc Natl Acad Sci U S A.* 2001;98(6):3346-3351.
50. Fabbri M, Iliopoulos D, Trapasso F, et al. WWOX gene restoration prevents lung cancer growth in vitro and in vivo. *Proc Natl Acad Sci U S A.* 2005;102(43):15611-15616.
51. Reid AH, Attard G, Ambroisine L, et al. Molecular characterisation of ERG, ETV1 and PTEN gene loci identifies patients at low and high risk of death from prostate cancer. *Br J Cancer.* 2010;102(4):678-684.
52. Wang J, Hua H, Ran Y, et al. Derlin-1 is overexpressed in human breast carcinoma and protects cancer cells from endoplasmic reticulum stress-induced apoptosis. *Breast Cancer Res.* 2008;10(1):R7.
53. Matolcsy A, Nador RG, Cesarman E, Knowles DM. Immunoglobulin VH gene mutational analysis suggests that primary effusion lymphomas derive from different stages of B cell maturation. *Am J Pathol.* 1998;153(5):1609-1614.
54. Carbone A, Cesarman E, Spina M, Gloghini A, Schulz TF. HIV-associated lymphomas and gamma-herpesviruses. *Blood.* 2009;113(6):1213-1224.
55. Khan G. Epstein-Barr virus and the germinal center B cells. *Exp Hematol.* 2006;34(6):695-696.
56. Johnson DR, Levan G, Klein G, Nigida SM Jr, Wolfe LG. Chromosomes and cell surface markers of marmoset lymphocytes and Epstein-Barr virus-transformed marmoset cell lines. *Cancer Genet Cytogenet.* 1981;3(2):101-108.
57. Vaghefi P, Martin A, Prevot S, et al. Genomic imbalances in AIDS-related lymphomas: relation with tumoral Epstein-Barr virus status. *AIDS.* 2006;20(18):2285-2291.
58. Chaudhary PM, Jasmin A, Eby MT, Hood L. Modulation of the NF-kappa B pathway by virally encoded death effector domains-containing proteins. *Oncogene.* 1999;18(42):5738-5746.
59. Brinkmann MM, Glenn M, Rainbow L, Kieser A, Henke-Gendo C, Schulz TF. Activation of mitogen-activated protein kinase and NF-kappaB pathways by a Kaposi's sarcoma-associated herpesvirus K15 membrane protein. *J Virol.* 2003;77(17):9346-9358.
60. Laherty CD, Hu HM, Opipari AW, Wang F, Dixit VM. The Epstein-Barr virus LMP1 gene product induces A20 zinc finger protein expression by activating nuclear factor kappa B. *J Biol Chem.* 1992;267(34):24157-24160.
61. Feske S. Calcium signalling in lymphocyte activation and disease. *Nat Rev Immunol.* 2007;7(9):690-702.
62. Dellis O, Arbabian A, Brouland JP, et al. Modulation of B-cell endoplasmic reticulum calcium homeostasis by Epstein-Barr virus latent membrane protein-1. *Mol Cancer.* 2009;8:59.
63. Bluteau O, Beaudoin JC, Pasturaud P, et al. Specific association between alcohol intake, high grade of differentiation and 4q34-q35 deletions in hepatocellular carcinomas identified by high resolution allelotyping. *Oncogene.* 2002;21(8):1225-1232.